J Radioanal Nucl Chem (2011) 288:121–130
DOI 10.1007/s10967-010-0895-8

Effect of environmental conditions on the sorption of radiocobalt from aqueous solution to treated eggshell as biosorbent

Shouwei Zhang · Zhiqiang Guo · Junzheng Xu · Haihong Niu · Zhesheng Chen · Jinzhang Xu

Received: 5 October 2010 / Published online: 2 November 2010

Abstract Carbonate hydroxylapatite (CHAP), prepared from eggshell waste, was used to remove ^{60}Co(II) from aqueous solutions. The sorption of ^{60}Co(II) on CHAP as a function of contact time, pH, ionic strength and foreign ions in the absence and presence of humic acid and fulvic acid under ambient conditions was studied. The sorption of ^{60}Co(II) on CHAP was strongly dependent on pH and ionic strength. The thermodynamic parameters (ΔH^0, ΔS^0, ΔG^0) of ^{60}Co(II) sorption on CHAP were calculated from the temperature-dependent sorption isotherms, and the results indicated that the sorption process of ^{60}Co(II) on CHAP was endothermic and spontaneous. At low pH, the sorption of ^{60}Co(II) was dominated by outer-sphere surface complexation and ion exchange with Na^+/H^+ on CHAP surfaces, whereas inner-sphere surface complexation was the main sorption mechanism at high pH. Experimental results also indicated that CHAP was a suitable low-cost adsorbent for pre-concentration and solidification of ^{60}Co(II) from large volumes of aqueous solutions.

Keywords Carbonate hydroxylapatite · Radiocobalt · pH · Sorption isotherm

Introduction

The physicochemical behavior of long-lived radionuclides are crucial to the environmental pollution [1, 2]. The presence of radionuclides in wastes is a major environmental concern. Such wastes arise from technologies producing nuclear fuels, and from laboratories working with radioactive materials [3].

^{60}Co(II) is one of the most serious radionuclides affecting the environment due to its long half-life ($T_{1/2} = 5.27a$). The radionuclides ^{60}Co and ^{58}Co are present in liquid wastes released from pressurized water nuclear power reactors [4]. High levels of ^{60}Co(II) may affect several health troubles such as paralysis, diarrhea, low blood pressure, lung irritation and bone defects [5]. The permissible limits of ^{60}Co(II) in the irrigation water and livestock wastewater are 0.05 and 1.00 mg/L, respectively [6]. Therefore, the elimination of radiocobalt from wastewaters is important to protect public health. The removal of radiocobalt from aqueous solution have been studied extensively [7–18]. Treatment processes for radionuclides contaminated water include chemical precipitation, membrane filtration, ion exchange, sorption, and co-precipitation/precipitation [19–22]. Among these methods, sorption process has been found as one of the most promising technologies in radionuclide pollution management because of its low cost, simplicity of design and operation [23–25].

Generally, activated carbon, carbon nanomaterials, clay minerals, silica gel, activated alumina and ion exchange resin have been widely used as adsorbents in the removal of radionuclides from large volume of aqueous solutions [26–31]. However, the high capital and regeneration cost of these materials limit their large-scale applications for the removal of radionuclides, which have encouraged researchers to look for low-cost alternative adsorbents [32–34]. The major advantages of biomaterial as sorbents are low cost, high efficiency, minimization of chemical or biological sludge, no additional nutrient requirement, possibility of regeneration of the biosorbent, and metal recovery [35–37]. Hydroxylapatite (HAP) as an efficient and low-cost biosorbent, which has high sorption ability for

S. Zhang · Z. Guo · J. Xu · H. Niu · Z. Chen · J. Xu (✉)
School of Nuclear Science and Technology, Lanzhou University, 730000 Lanzhou, People's Republic of China
e-mail: xujz@lzu.edu.cn

^{60}Co(II). HAP was found to have high removal efficiency for the retention of Cd, Zn and Co in a wide pH range of 6–9 [38]. The interaction of Co^{2+} with HAP was also studied from the aspect of the catalytic activities of cobalt/calcium exchanged samples for oxidative dehydrogenation of ethane [39].

It is well-known that HAP can be prepared from a variety of raw materials. The most frequently used precursors are animal bones [40, 41] and coral [42]. Eggshell waste is widely produced from houses, restaurants, and bakeries. Eggshell has a little developed porosity and pure $CaCO_3$ as an important constituent. In this work, carbonate hydroxylapatite (CHAP) was synthesized by using eggshell from the viewpoint of recycling this waste product and minimization of contaminants. The properties of the prepared CHAP from eggshells were determined, and the potential use of CHAP in the removal of ^{60}Co(II) was studied.

The main purposes of this study are: (1) to investigate the sorption kinetics of ^{60}Co(II) on CHAP and to analyze the experimental data with a pseudo-second-order equation; (2) to study the sorption of ^{60}Co(II) on CHAP as a function of pH, ionic strength, foreign ions in the absence and presence of HA/FA; (3) to calculate the thermodynamic parameters (i.e., ΔH^0, ΔS^0, ΔG^0) from the temperature dependent sorption isotherms; and (4) to presume the sorption mechanisms of ^{60}Co(II) on CHAP.

Experimental section

Preparation of CHAP

The eggshell samples used in this study were obtained from some private restaurant in China. CHAP samples were prepared as: the eggshells were washed with distilled water for several times to remove impurity and interference material such as organics and salts. Then, they were transferred to the oven at 70 °C to dry. The pretreated eggshells were calcined in air using a muffle furnace at 900 °C (heating rate of 10 °C/min) for 1 h. The following reaction happened in the calcinations:

$$CaCO_3 \xrightarrow{900\,^{\circ}C} CaO + CO_2 \uparrow \quad (1)$$

The calcined powder was ground in an alumina mortar-pestle. This CaO powder was completely dissolved in concentrated H_3PO_4, kept at 30–40 °C for 2–3 h, under pH 3.0. The following reaction happened in the acidic conditions:

$$CaO + H_3PO_4 = CaHPO_4 + H_2O \quad (2)$$

Insoluble material was separated and removed by filtration. Subsequently, 1 mol/L $Ca(OH)_2$ was added into the solution, kept at 100 °C for 24 h, adjusting pH to 11.0 by using 0.1 mol/L NaOH. When it was naturally cooled to room temperature, the suspension was collected by filtration, and washed thoroughly with distilled water to remove the excrescent free ions, and at last rinsed with distilled water until the pH of the solution reached to about 7.0. The reaction processed following the equation:

$$CaHPO_4 + CO_2 + Ca(OH)_2 \rightarrow Ca_{10}\left\{(PO_4)_{6-x}, (CO_3 \cdot OH)_x\right\}(OH)_2 \quad (3)$$

Finally, the sample was dried at 60 °C for 24 h and ground to pass 200 meshes to get the CHAP samples.

All chemicals used in the experiments were purchased as analytical purity and used directly without any further purification. All the reagents were prepared with high-purity Milli-Q water from a Millipore Synthesis A10 water system (18.2 MΩ).

Sorption experiments

All the experiments were carried out in polyethylene centrifuge tubes by using batch technique under ambient conditions. The stock suspension of CHAP was pre-equilibrated with $NaClO_4$ solution for 24 h, and then ^{60}Co(II) stock solution was added into the polyethylene test tubes to achieve the desired concentrations of different components. The pH values of the systems were adjusted by adding negligible volume of 0.1 or 0.01 mol/L $HClO_4$ or NaOH. After the suspensions were shaken for 24 h, the solid and liquid phases were separated by centrifugation at 9000 rpm for 30 min at the temperature controlled same to that in the sorption experiments. It was necessary to note that the sorption of ^{60}Co(II) on the tube wall was negligible according to the test of ^{60}Co(II) sorption in the absence of CHAP.

The concentration of radionuclide ^{60}Co(II) was analyzed by liquid scintillation counting using a Packard 3100 TR/AB Liquid Scintillation Analyzer (PerkinElmer). The scintillation cocktail was ULTIMA GOLD AB™ (Packard). The amount of ^{60}Co(II) adsorbed on CHAP was calculated from the difference between the initial concentration (C_0) and the equilibrium one (C_e). The sorption of ^{60}Co(II) was expressed in terms of *sorption percentage* (%):

$$\text{Sorption}(\%) = \frac{C_0 - C_e}{C_0} \times 100\% \quad (4)$$

All experiment date were the average of triplicate determinations and the relative errors were about 5%.

Results and discussion

Kinetic sorption of ^{60}Co(II) on CHAP

The sorption of ^{60}Co(II) on CHAP as a function of contact time was investigated at pH = 6.5 ± 0.1 (Fig. 1). It

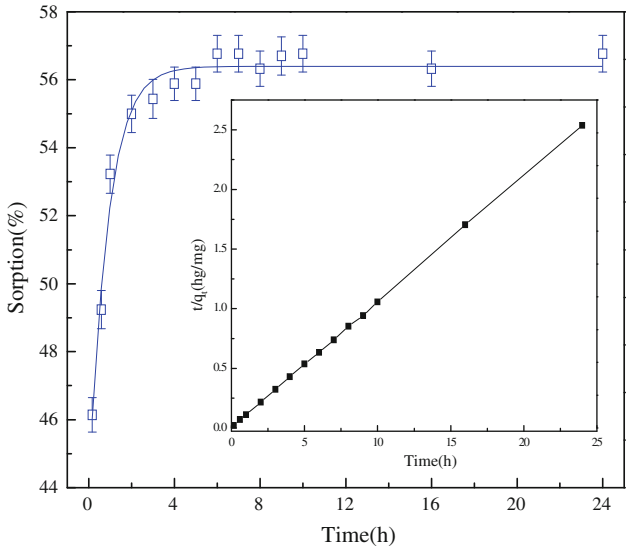

Fig. 1 Effect of contact time on ^{60}Co(II) sorption on CHAP and the pseudo-second-order rate equation fit (*inset*), pH = 6.5 ± 0.1, I = 0.01 mol/L $NaClO_4$, T = 303.15 K, m/V = 0.6 g/L, $C_{Co(II)initial}$ = 1.67×10^{-4} mol/L

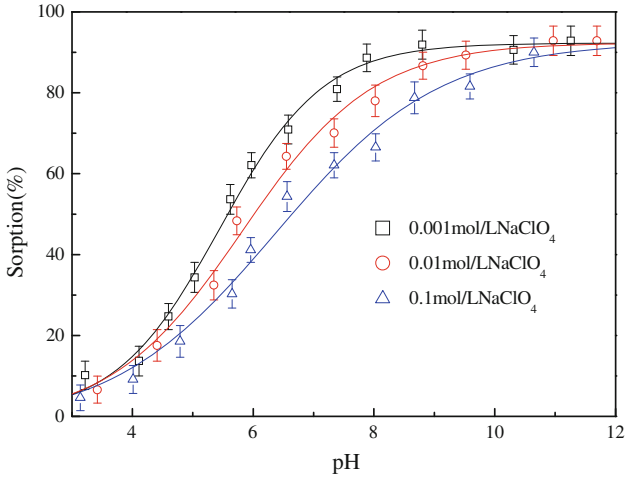

Fig. 2 Effect of ionic strength on ^{60}Co(II) sorption on CHAP as a function of pH, T = 303.15 K, m/V = 0.6 g/L, $C_{Co(II)initial}$ = 1.67×10^{-4} mol/L

seemed that the sorption consisted of two phases: a primary rapid phase and a second slow phase. The first rapid phase lasted approximately 2 h and accounted for the major part in the total ^{60}Co(II) sorption. Sorption reached a plateau value in approximately 4 h, which showed saturation of the active points. According to the above results, the shaking time was fixed to 24 h for the rest of the batch experiments to assure the sorption equilibrium.

In order to analyze the sorption rate of ^{60}Co(II) on CHAP, the pseudo-second-order rate equation is used to simulate the kinetic sorption [43, 44]:

$$\frac{t}{q_t} = \frac{1}{2Kq_e^2} + \frac{1}{q_e}t \tag{5}$$

where q_t (mg/g) is the amount of ^{60}Co(II) adsorbed on CHAP at time t, and q_e (mg/g) is the equilibrium sorption capacity. K (g/(mg h)) is the pseudo-second-order rate constant.

Constant K and q_e were calculated from the intercept and slope of the line obtained by plotting t/q_t vs. t (the inserted figure in Fig. 1). The value of pseudo-second-order rate constant K is 0.958 *g/*(mg h) and the equilibrium sorption capacity q_e is 9.479 mg/g. The correlation coefficient (R^2 = 0.999) of the linear plot is very close to 1, which suggests that the experimental data can be fitted very well by the pseudo-second-order model [45–47].

Effect of pH and ionic strength

The pH-dependent sorption of ^{60}Co(II) on CHAP as a function of ionic strength is shown in Fig. 2. It is clear that sorption of ^{60}Co(II) on CHAP is obviously affected by solution pH values. The sorption of ^{60}Co(II) increases abruptly from ~10 to ~93% at pH 4.0–10.5, and approaches a plateau at pH > 10.5. There are two possible reactions for the removal of ^{60}Co(II) from aqueous solutions [48]. The first mechanism is the sorption of ^{60}Co(II) on the surfaces by ion exchange. The ion exchange can be expressed as follow:

$$Co^{2+}_{(s)} + \equiv S{-}O{-}Ca^{2+}_{(C)} \rightarrow \equiv S{-}O{-}Co^{2+}_{(C)} + Ca^{2+}_{(s)} \tag{6}$$

$$Co^{2+}_{(s)} + 2 \equiv S{-}O{-}Na^{+}_{(C)} \rightarrow (\equiv S{-}O)_2{-}Co^{2+}_{(C)} + 2Na^{+}_{(s)} \tag{7}$$

where subscripts (s) and (C) denote solution and CHAP phase, respectively.

The second mechanism is surface complexation by CHAP. The surface functional groups of CHAP participate in the formation of complexes in the removal of Co(II) tom CHAP.

It is generally regarded that the species of ^{60}Co(II) in solution are important to ^{60}Co(II) sorption. The species of ^{60}Co(II) are strongly dependent on pH values. Figure 3 shows the relative distribution of ^{60}Co(II) species calculated from the stability constants ($\log K_1 = -9.6$, $\log K_2 = -9.2$, and $\log K_3 = -12.7$) [49]. The results demonstrate that ^{60}Co(II) presents in the forms of Co^{2+}, $Co(OH)^+$, $Co(OH)_2$ and $Co(OH)_3^-$ at various pH values. At pH < 7.5, the main species of ^{60}Co(II) is Co^{2+}, and ^{60}Co(II) does not form precipitation in this pH region. In the pH > 7.5, $Co(OH)^+$ and $Co(OH)_3^-$ become the main species. In the pH > 10.5, Co^{2+} mainly forms precipitation. At pH < 7.5, the predominant species is Co^{2+}. Due to the protonation reaction (i.e., $\equiv SOH + H^+ \leftrightarrow \equiv SOH_2^+$) on the surfaces of CHAP, the concentration of protonated

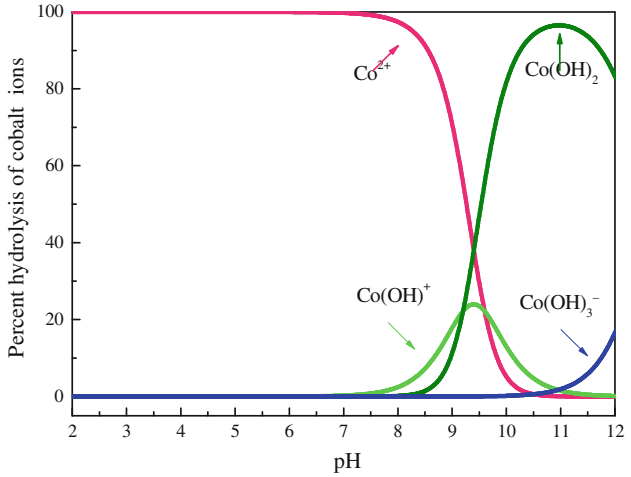

Fig. 3 Relative proportion of ^{60}Co(II) species as a function of pH

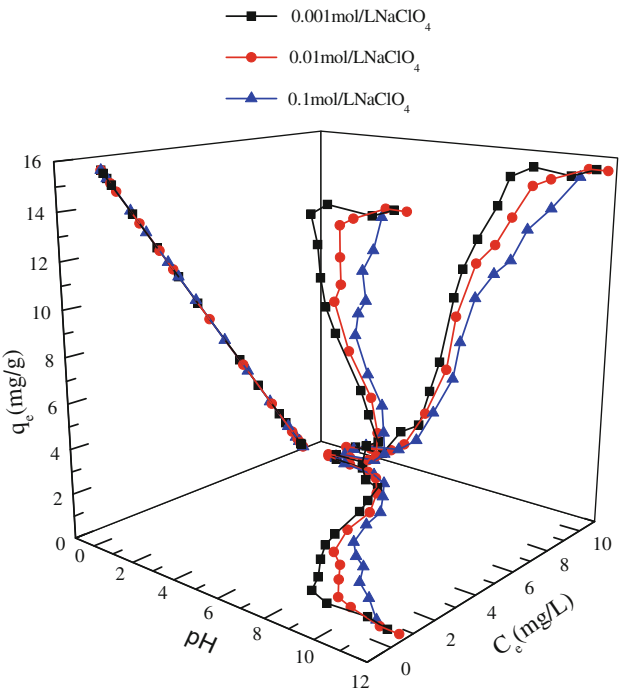

Fig. 4 3D plots of pH, C_e and q_e of ^{60}Co(II) sorption on CHAP, $T = 303.15$ K, $m/V = 0.6$ g/L, $C_{Co(II)initial} = 1.67 \times 10^{-4}$ mol/L

sites ($\equiv SOH_2^+$) decreases with increasing pH. Thereby, the sorption of Co^{2+} is unfavorable as a result of coulombic repulsion at pH range 1.0–4.0. However, at high pH values, the concentration of deprotonated sites ($\equiv SOH^-$) increases with increasing pH because of the surface deprotonation reaction (i.e., $\equiv SOH \leftrightarrow \equiv SO^- + H^+$). The deprotonated sites ($\equiv SOH^-$) are more available to retain the metal ions and surface complexation between Co^{2+} and CHAP is facilitated, thus resulting in sharp increase of ^{60}Co(II) sorption at pH 4.0–10.5.

Figure 2 also shows the effect of ionic strength on ^{60}Co(II) sorption to CHAP. It is well known that ClO_4^- does not form complexes with ^{60}Co(II) in solution or on CHAP surfaces. The influence of $NaClO_4$ concentration on ^{60}Co(II) sorption is mainly due to the competition of Na^+ with ^{60}Co(II) on CHAP surfaces. One can see that the sorption of ^{60}Co(II) at pH < 10.5 is influenced by ionic strength obviously, whereas no drastic difference of ^{60}Co(II) sorption to CHAP is found at pH > 10.5. The pH- and ionic strength-dependent sorption of ^{60}Co(II) at pH < 10.5 suggests that the removal of ^{60}Co(II) to CHAP is dominated by ion exchange or outer-sphere surface complexation, whereas the pH-dependent and ionic strength-independent ^{60}Co(II) sorption indicates that the sorption of ^{60}Co(II) is mainly due to inner-sphere surface complexation or surface precipitation at pH > 10.5 [50–54].

To illustrate the variation and relationship of C_e, pH and q_e (mg/g, the concentration of ^{60}Co(II) on solid phase), the experimental data of ^{60}Co(II) sorption in 0.001, 0.01 and 0.1 mol/L $NaClO_4$ were plotted as 3D plots of C_e, pH and q_e (Fig. 4). On the pH–q_e plane, one can see that the lines are very similar to those of pH-sorption percentages (in Fig. 2); On the pH–C_e plane, the projection on the pH–C_e plane is just the inverted image of the projection on the pH–q_e plane; On the C_e–q_e plane, the projection is a straight line containing all experimental data, which is due to the same initial concentration of ^{60}Co(II) for each experimental point. The following equation can describe the relationship of C_e–q_e:

$$VC_0 = mq_e + VC_e \tag{8}$$

Equation 8 can be rearranged as:

$$q_e = C_0\frac{V}{m} - C_e\frac{V}{m} \tag{9}$$

where V is the volume and m is the mass of CHAP. Thereby, the experimental data of C_e–q_e lies in a straight line with slope ($-V/m$) and intercept (C_0V/m). The slope and the intercept calculated from C_e to q_e line are -1.67 and 16.67, which are quite in accordance with the values of $V/m = 1.67$ L/g and $C_0V/m = 16.67$ mg/g. The 3D plots show the relationship of C_e, pH and q_e very clearly, i.e., all the data of C_e–q_e lie in a straight line with slope $-V/m$ and intercept C_0V/m at same initial concentrations and same solid contents [55, 56].

Effect of foreign ions

In order to investigate the influence of background electrolyte ions on ^{60}Co(II) sorption, the sorption of ^{60}Co(II) on CHAP was studied as a function of pH values in 0.01 mol/L $NaClO_4$, NaCl, $NaNO_3$, $KClO_4$ and $LiClO_4$, respectively. Figure 5a shows that the sorption of ^{60}Co(II)

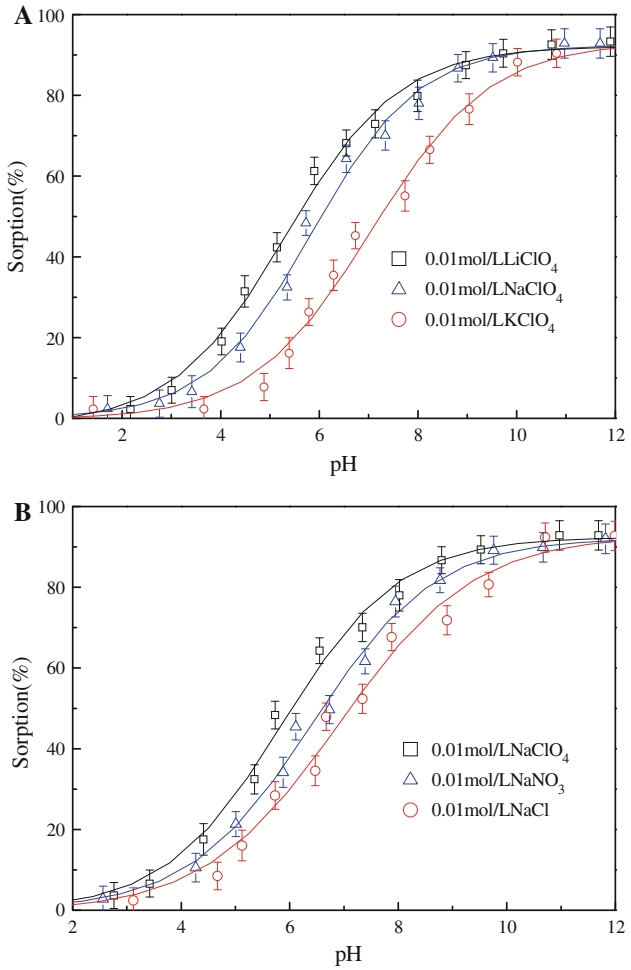

Fig. 5 Effect of foreign ions on ^{60}Co(II) sorption on CHAP as a function of pH, $T = 303.15$ K, $m/V = 0.6$ g/L, $C_{\text{Co(II)initial}} = 1.67 \times 10^{-4}$ mol/L

on CHAP is clearly influenced by the cations in the suspension. At pH < 10.5, the sorption percentage of ^{60}Co(II) on CHAP under the same pH values are in the following sequence: $Li^+ > Na^+ > K^+$, indicating that the cations can alter the surface property of CHAP, and thus can influence the sorption of ^{60}Co(II) on CHAP [57]. The sorption of ^{60}Co(II) on CHAP can be considered as a competition of ^{60}Co(II) with Li^+ (or Na^+, K^+) at CHAP surfaces. The hydration radius of the three cations is $K^+ = 2.32$ Å, $Na^+ = 2.76$ Å and $Li^+ = 3.4$ Å [58, 59]. The hydration radio of K^+ is smaller than those of the other two cations and therefore the influence of K^+ on ^{60}Co(II) sorption is more obvious than those of Na^+ and Li^+. However, at pH > 10.5, no drastic difference of ^{60}Co(II) sorption to CHAP in $LiClO_4$, $NaClO_4$ and $KClO_4$ solutions is observed, which may be attributed to the inner-sphere surface complexation or surface precipitatation at high pH values. Esmadi and Simm [59] investigated the effect of Li^+, Na^+ and K^+ on the sorption of ^{60}Co(II) to amorphous ferric hydroxide and similar results were also found. Xu et al. [60] studied the sorption of Th(IV) on rectorite and also found similar results.

From Fig. 5b, one can see that the sorption of ^{60}Co(II) on CHAP is influenced by the background electrolyte anions. The effect of anions on the sorption of ^{60}Co(II) to CHAP under the same pH values is in the following sequence: $ClO_4^- > NO_3^- > Cl^-$. This phenomenon might be attributed to the facts that: (1) idiocratic sorption of Cl^- to CHAP surface is a little easier than NO_3^- and ClO_4^-, and Cl^- sorption on the surface of CHAP changes the surface properties of CHAP and decreases the availability of binding sites for ^{60}Co(II); (2) Cl^- and NO_3^- can form soluble complexes with ^{60}Co(II) (e.g., $CoCl^+$ and $CoNO_3^+$), whereas ClO_4^- can not. ^{60}Co(II) has higher affinity with Cl^- than NO_3^- and ClO_4^-; and (3) the inorganic acid radical radius order is $ClO_4^- > NO_3^- > Cl^-$, the smaller radius of inorganic acid radicals takes up more ionic exchange sites and results in the decrease of ^{60}Co(II) sorption on CHAP [28].

Effect of HA/FA

The sorption of ^{60}Co(II) on CHAP in the absence and presence of humic acid (HA) and fulvic acid (FA) as a function of pH is shown in Fig. 6. It is very interesting to notice that the presence of FA/HA decreases the sorption of ^{60}Co(II) on HA/FA-CHAP hybrids at pH < 11.0. The surface charge of CHAP is negative and the sorption of negatively charged HA/FA on the negatively charged CHAP surface decreases with increasing pH due to electrostatic repulsion [61–63]. This causes the formation of soluble complexes of HA/FA-^{60}Co(II) in solution, and the

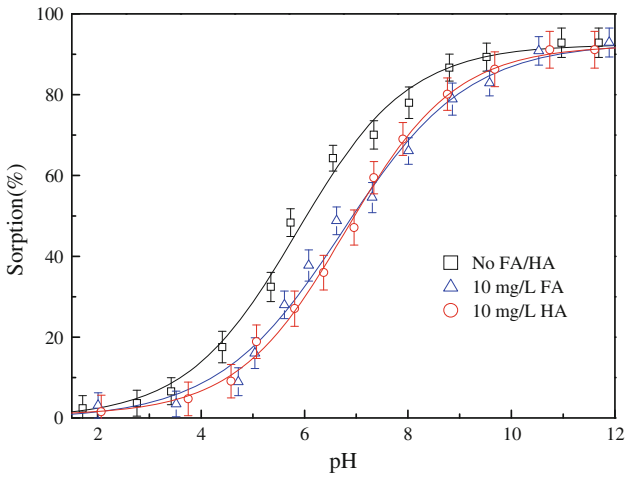

Fig. 6 Effect of HA/FA on ^{60}Co(II) sorption on CHAP as a function of pH, $T = 303.15$ K, $m/V = 0.6$ g/L, $C_{\text{HA}} = 10$ mg/L, $C_{\text{FA}} = 10$ mg/L, $C_{\text{Co(II)initial}} = 1.67 \times 10^{-4}$ mol/L

strong complexation ability of HA/FA with ^{60}Co(II) results in the decrease of ^{60}Co(II) sorption [64]. The negative effect of HA/FA on ^{60}Co(II) sorption to HA/FA-CHAP is different to most metal ion sorption to HA/FA bound materials [56, 65–69]. In the studies mentioned above, the surface charge of the materials is positive at low pH and the sorption of HA/FA on the positively charged surface of solid particle is high. The surface adsorbed HA/FA forms strong surface complexes with radionuclides on solid surfaces, and thereby enhances the sorption of radionuclides at low pH values [70–72]. At pH > 11.0, one can see that there is no drastic difference in the sorption of ^{60}Co(II) on bare and HA/FA-bound CHAP particles. The influence of HA/FA on ^{60}Co(II) sorption at pH > 11.0 can be negligible because of the high sorption or precipitation of ^{60}Co(II) at CHAP surfaces. The chemical bonds between ^{60}Co(II) and the surface functional groups of CHAP or HA/FA functional groups may be very similar at pH > 11.0. The influence of HA/FA on Co(II) sorption is also dependent on the macromolecular structures of HA/FA and the sorption ability of Co(II) with CHAP at different pH values. At low pH values, the sorption of Co(II) on CHAP is weaker than that of Co(II) with HA/FA, whereas the sorption of Co(II) on CHAP is much strong at high pH and the presence of FA/HA can not affect Co(II) sorption on CHAP obviously [73, 74].

It is very interesting to find that the sorption curve of ^{60}Co(II) to CHAP in the presence of HA is quite similar to that of ^{60}Co(II) to CHAP in the presence of FA. HA and FA are chemically heterogeneous compounds that contain different types of functional groups at different proportions and configurations. HA and FA contain carboxyl groups, amine groups and phenolic groups [63], and these functional groups play an important role in affecting ^{60}Co(II) sorption to CHAP. The samples of HA and FA were extracted from the same soil samples, and thus they might have similar functional groups such as carboxyl and phenolic groups. As is illustrated in Table 1, the quantitative concentrations of functional groups of HA are very similar to that of FA. It is clearly observed in Fig. 6 that the influence of HA is very similar to that of FA. These similar functional groups and sorption property of HA and FA may interpret the similar sorption curve of ^{60}Co(II) to CHAP in the presence of HA/FA.

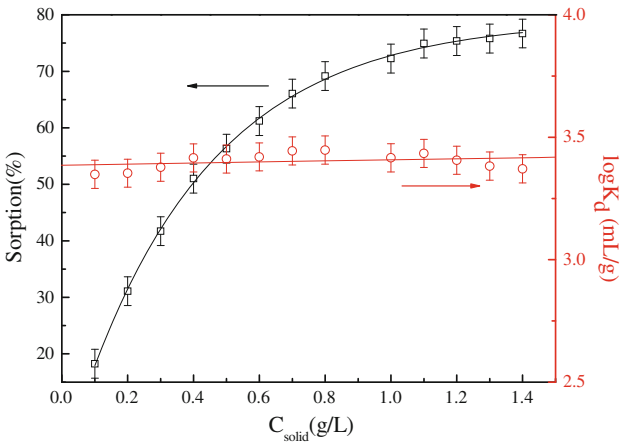

Fig. 7 Effect of solid content on ^{60}Co(II) sorption on CHAP, pH = 6.5 ± 0.1, I = 0.01 mol/L $NaClO_4$, T = 303.15 K, $C_{Co(II)initial}$ = 1.67 × 10^{-4} mol/L

Effect of CHAP content

The sorption of ^{60}Co(II) on CHAP as a function of CHAP content is shown in Fig. 7. The distribution coefficient, K_d, value as a function of the CHAP content is also plotted in Fig. 7.

The distribution coefficient (K_d) value was derived from the following equation:

$$K_d = \frac{C_0 - C_e}{C_e}\frac{V}{m} \tag{10}$$

where C_0 and C_e are defined above, m is the mass of adsorbent (g), and V is the volume of the suspension (L).

One can see that the removal of ^{60}Co(II) from solution to CHAP increases with increasing CHAP content. With increasing solid content, more surface sites is available to bind ^{60}Co(II) at CHAP. Thereby, more ^{60}Co(II) ions are adsorbed on CHAP at high solid content. The K_d maintains a level with increasing CHAP content, which is in consistent with the physicochemical properties of the distribution coefficient, i.e., the K_d value is independent of solid content at low solid and liquid concentrations [75, 76].

Effect of temperature and thermodynamic study

Figure 8 shows the sorption isotherms of ^{60}Co(II) on CHAP at three different temperatures. One can see that the

Table 1 The concentrations of functional groups of HA and FA calculated from potentiometric titration by using FITEQL 3.1

	Log K_a			C(mol/g)			Surface sites density (mol/g)	WSOS/DF
	L_1	L_2	L_3	HL_1	HL_2	HL_3		
HA	−5.04	−7.40	−9.60	2.20 × 10^{-3}	1.08 × 10^{-3}	3.18 × 10^{-3}	6.46 × 10^{-3}	2.37
FA	−5.19	−7.77	−10.53	1.83 × 10^{-3}	1.08 × 10^{-3}	2.42 × 10^{-2}	2.71 × 10^{-2}	0.10

HL_1, *HL_2* and *HL_3* present the carboxyl groups (–COOH), the phenolic (Ar–OH) and the amine groups (–NH_2) of HA and FA, respectively

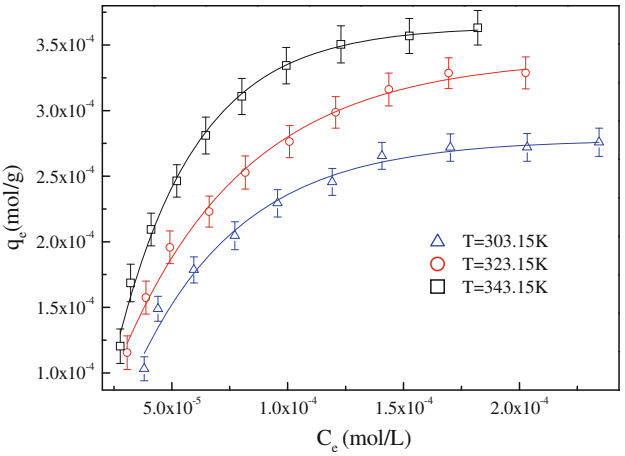

Fig. 8 Sorption isotherms of ^{60}Co(II) on CHAP at three different temperatures, $I = 0.01$ mol/L $NaClO_4$, pH = 6.5 ± 0.1, $m/V =$ 0.6 g/L

sorption isotherm is the highest at $T = 343.15$ K and is the lowest at $T = 303.15$ K, which indicates that the sorption of ^{60}Co(II) on CHAP is promoted at higher temperature. It is reasonable that the sorption of ^{60}Co(II) increases with increasing temperature. Several factors may account for this phenomenon. Increased diffusion rate of adsorbate molecules into the CHAP pores due to increased temperature may account for the observed behavior [77]. Changes in the adsorbent pore sizes as well as an increase in the number of sorption sites due to the breaking of some internal bonds near the edge of the particle are expected at higher temperatures [78]. An increase in temperature may also affect an increase in proportion and activity of ^{60}Co(II) in solution, the affinity of the ions to the surface, and therefore affect the potential of the surface [79, 80].

Three different models, viz. Langmuir, Freundlich and D–R isotherm equations, are employed to simulate the sorption isotherms and to establish the relationship between the amount of ^{60}Co(II) adsorbed on solid phase and the concentration of ^{60}Co(II) remaining in solution.

The Langmuir isotherm model is used to describe the monolayer sorption process. It can be represented by the following equation [63, 81]:

$$q_e = \frac{bq_{max}C_e}{1 + bC_e} \tag{11}$$

Equation 11 can be expressed in linear form:

$$\frac{C_e}{q_e} = \frac{1}{bq_{max}} + \frac{C_e}{q_{max}} \tag{12}$$

where C_e is the equilibrium concentration of ^{60}Co(II) remained in solution (mol/L); q_e is the amount of ^{60}Co(II) adsorbed on per weight unit of solid after equilibrium (mol/g); q_{max} is the amount of ^{60}Co(II) at complete

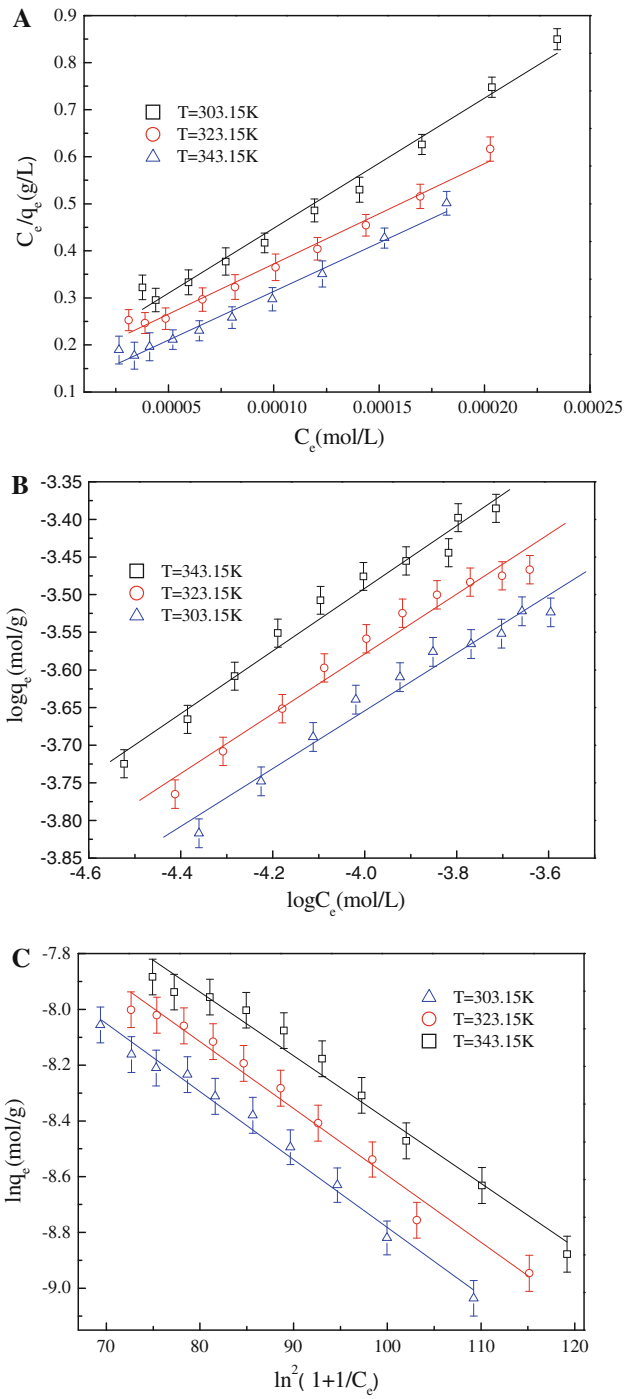

Fig. 9 Langmuir (**a**), Freundlich (**b**) and D–R (**c**) isotherm for ^{60}Co(II) sorption on CHAP at three different temperatures, $I = 0.01$ mol/L $NaClO_4$, pH = 6.5 ± 0.1, $m/V = 0.6$ g/L

monolayer coverage (mol/g) and b (L/mol) is a constant that relates to the heat of sorption.

The Freundlich isotherm model allows for several kinds of sorption sites on the solid surface and represents properly the sorption data at low and intermediate

concentrations on heterogeneous surfaces [82]. The model has the following form:

$$q_e = k_F C_e^n \tag{13}$$

Equation 14 can be expressed in linear form:

$$\log q_e = \log k_F + n \log C_e \tag{14}$$

where k_F ($mol^{1-n}\ L^n/g$) represents the sorption capacity and n represents the degree of dependence of sorption with equilibrium concentration.

The D–R isotherm model is more general than the Langmuir isotherm since it does not assume a homogeneous surface or constant sorption potential [59, 83]. The D–R equation has the general expression:

$$q_e = q_{max} \exp(-\beta\varepsilon^2) \tag{15}$$

Equation 15 can be expressed in linear form:

$$\ln q_e = \ln q_{max} - \beta\varepsilon^2 \tag{16}$$

where q_e and q_{max} are defined above, β is the activity coefficient related to the mean sorption energy (mol^2/kJ^2), and ε is the Polanyi potential, which is equal to:

$$\varepsilon = RT \ln\left(1 + \frac{1}{C_e}\right) \tag{17}$$

where R is ideal gas constant (8.314 J/(mol K)), and T is the absolute temperature in Kelvin (K).

The experimental data of ^{60}Co(II) sorption are analyzed with the Langmuir, Freundlich and D–R models, and the results are shown in Fig. 9. The relative values calculated from the three models are listed in Table 2. It can be concluded from the correlation coefficients that Langmuir model simulates the experimental data better than Freundlich and similar to D–R models. The fact that the Langmuir isotherm fits the experimental data very well suggests almost complete monolayer coverage of the adsorbent particles. Moreover, CHAP has a limited sorption capacity, thus the sorption could be better described by Langmuir model than by Freundlich, since an exponentially increasing sorption was assumed in the Freundlich model [8]. The values of q_{max} obtained from the Langmuir model for ^{60}Co(II) sorption on CHAP are the highest at $T = 343.15$ K and the lowest at $T = 303.15$ K, which indicates that the sorption is enhanced with increasing temperature. In the Freundlich model, the value of n is from unity, which indicates that a nonlinear sorption takes place on the heterogeneous surfaces. The sorption capacities q_{max} derived from the D–R model are higher than those derived from the Langmuir model. This may be ascribed to the different assumptions considered in the formulation of the isotherms [30, 45].

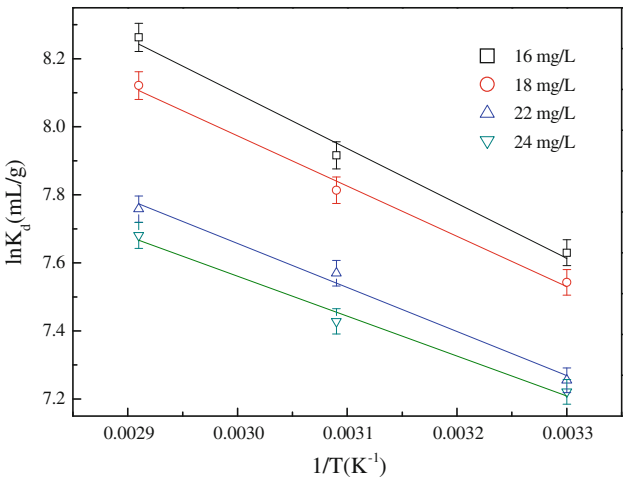

Fig. 10 Linear plots of $\ln K_d$ versus $1/T$ for ^{60}Co(II) sorption on CHAP at three different temperatures, $I = 0.01$ mol/L $NaClO_4$, pH = 6.5 ± 0.1, $m/V = 0.6$ g/L

The thermodynamic parameters (ΔH^0, ΔS^0 and ΔG^0) for ^{60}Co(II) sorption on CHAP are calculated from the temperature dependent sorption isotherms. The values of enthalpy (ΔH^0) and entropy (ΔS^0) can be calculated from the slope and intercept of the plot of $\ln K_d$ vs. $1/T$ (Fig. 10):

$$\ln K_d = \frac{\Delta S^0}{R} - \frac{\Delta H^0}{RT} \tag{18}$$

where R and T are defined above. The Gibbs free energy change (ΔG^0) is calculated from the following equation:

$$\Delta G^0 = \Delta H^0 - T\Delta S^0 \tag{19}$$

The values obtained from Eqs. 18 and 19 are tabulated in Table 3. The evaluation of thermodynamic parameters provides an insight into the mechanism of ^{60}Co(II) sorption to CHAP. As is expected for a spontaneous process under

Table 2 The parameters for Langmuir, Freundlich and D–R sorption isotherms of ^{60}Co(II) on CHAP at different temperatures

T (K)	Langmuir			Freundlich			D–R		
	q_{max} (mol/g)	b (L/mol)	R	K_F ($mol^{1-n}\ L^n/g$)	n	R	β(mol^2/kJ^2)	q_{max}(mol/g)	R
303.15	3.61×10^{-4}	1.61×10^4	0.982	7.64×10^{-3}	0.384	0.967	3.83×10^{-3}	1.18×10^{-3}	0.985
323.15	4.69×10^{-4}	1.34×10^4	0.984	1.03×10^{-2}	0.397	0.965	3.32×10^{-3}	2.04×10^{-3}	0.981
343.15	4.83×10^{-4}	1.94×10^4	0.981	1.49×10^{-2}	0.416	0.974	2.81×10^{-3}	2.23×10^{-3}	0.975

Table 3 Values of thermodynamic parameters for the sorption of ^{60}Co(II) on CHAP

C_0 (mg/L)	ΔH^0 (kJ/mol)	ΔS^0 (J/(mol K))	ΔG^0 (kJ/mol)		
			303.15 K	323.15 K	343.15 K
10	13.43	107.62	−19.19	−21.35	−23.50
12	12.29	103.16	−18.98	−21.05	−23.11
14	10.77	95.96	−18.32	−20.24	−22.16
16	9.76	92.13	−18.17	−20.02	−21.86

the experimental conditions, it is clear that the Gibbs free energy change (ΔG^0) of ^{60}Co(II) sorption on CHAP is more negative at higher temperature, which demonstrates that the spontaneity of the sorption process increases with the rise in temperature. At high temperature, cations are readily desolvated and hence its sorption becomes more favorable. A positive value of the standard enthalpy change (ΔH^0) indicates that the sorption process is endothermic. The positive ΔS^0 value suggests the affinity of CHAP toward ^{60}Co(II) ions in aqueous solutions and may suggest some structure changes on the sorbents [28].

Conclusions

In this study, batch technique was adopted to investigate the sorption of ^{60}Co(II) from simulated wastewater onto CHAP as a function of various environmental factors such as contact time, pH, ionic strength, coexisting electrolyte ions, humic substances and temperature under ambient conditions. The sorption percentage of ^{60}Co(II) weakly increases with increasing pH values at pH < 4.0, sharply increasing at $4.0 <$ pH < 10.5, and then maintains the high level at pH > 10.5. The sorption of ^{60}Co(II) is dependent on ionic strength at low pH values, and independent of ionic strength at high pH values. The thermodynamic analysis derived from temperature dependent sorption isotherms suggests that the sorption process of ^{60}Co(II) on CHAP is spontaneous and endothermic. By integrating all the above-mentioned analysis, one can conclude that the sorption of ^{60}Co(II) on CHAP is dominated by ion exchange or outer-sphere surface complexation at low pH values, and by inner-sphere surface complexation or precipitation at high pH values. Considering low cost, accessibility, ubiquitous presence in catering industry and large-scale applications of eggshell, one can conclude that CHAP, which is prepared by eggshell waste, has a great application potential for cost-effective material for ^{60}Co(II) preconcentration from large volumes of aqueous solutions.

Acknowledgments Financial support from the 973 project (2008CB417212) is acknowledged.

References

1. Shao DD, Xu D, Wang SW, Fan QH, Wu WS, Dong YH, Wang XK (2009) Sci China B: Chem 52:362–371
2. Fan QH, Shao DD, Hu J, Chen CL, Wu WS, Wang XK (2009) Radiochim Acta 97:141–148
3. Humeinicu D, Drochioiu G, Popa K (2004) J Radioanal Nucl Chem 260:291–293
4. Yu SM, Li XG, Ren AP, Shao DD, Chen CL, Wang X (2006) J Radioanal Nucl Chem 268(2):387–392
5. Kudesia VP (1990) Water pollution. Pragati parkashan, Meerut
6. Rengaraj S, Moon SH (2002) Water Res 36:1783–1793
7. Yu SM, Ren AP, Chen CL, Chen YX, Wang XK (2006) Appl Radiat Isot 64:455–461
8. Chen CL, Xu D, Tan XL, Wang XK (2007) J Radioanal Nucl Chem 273:227–233
9. Yu SM, Ren AP, Cheng J, Song XP, Chen C, Wang X (2007) J Radioanal Nucl Chem 273:129–133
10. Chen L, Yu XJ, Zhao ZD, Pan JS (2008) J Radioanal Nucl Chem 275:209–216
11. Khan SA (2003) J Radioanal Nucl Chem 258:3–6
12. El-Khouly SH (2006) J Radioanal Nucl Chem 270:391–398
13. Lopez H, Olguin MT, Bosch P, Bulbulian S (1995) J Radioanal Nucl Chem 200:19–23
14. Khan SA, Rehman RU, Khan MA (1996) J Radioanal Nucl Chem 207:19–37
15. Shakir K, Flex H, Benyamin K (1993) J Radioanal Nucl Chem 173:303–311
16. Shahwan T, Erten HN (1999) J Radioanal Nucl Chem 241:151–155
17. Dong WM, Wang XK, Shen Y, Zhao XD, Tao ZY (2000) J Radioanal Nucl Chem 245:431–434
18. Todorov B, Pekov G, Djingova R (2008) J Radioanal Nucl Chem 278:9–15
19. Bailey SE, Olin TJ, Bricka RM, Adrian DD (1999) Water Res 33:2469–2479
20. Tan XL, Fang M, Chen CL, Yu SM, Wang XK (2008) Carbon 46(13):1741–1750
21. Chen CL, Hu J, Xu D, Tan XL, Meng YD, Wang XK (2008) J Colloid Interf Sci 323:33–41
22. Xu D, Tan XL, Chen CL, Wang XK (2008) Appl Clay Sci 41:37–46
23. Faust SD, Aly OM (1987) Adsorption process for water treatment. Butterworths Publishers, Stoneham
24. Xu D, Zhou X, Wang XK (2008) Appl Clay Sci 39:133–141
25. Shao DD, Jiang ZQ, Wang XK, Li JX, Meng YD (2009) J Phys Chem B 113(4):860–864
26. Chen CL, Hu J, Shao DD, Li JX, Wang XK (2009) J Hazard Mater 164:923–928
27. Tan XL, Fang M, Li JX, Lu Y, Wang XK (2009) J Hazard Mater 168:458–465
28. Yang ST, Li JX, Shao DD, Hu J, Wang XK (2009) J Hazard Mater 166:109–116
29. Tan XL, Chang PP, Fan QH, Zhou X, Yu SM, Wu WS, Wang XK (2008) Colloid Surf A 328:8–14
30. Tan XL, Wang XK, Fang M, Chen CL (2007) Colloid Surf A 296:109–116
31. Zhao GX, Zhang HX, Fan QH, Ren XM, Li JX, Chen YX, Wang XK (2010) J Hazard Mater 173:661–668
32. Babel S, Kurniawan TA (2003) J Hazard Mater B97:219–243
33. Dias JM, Alvim-Ferraz MCM, Almeida MF, Rivera-Utrilla J, Sanchez-Polo M (2007) J Environ Manage 85:833–846
34. Fan QH, Shao DD, Hu J, Wu WS, Wang XK (2008) Surf Sci 602:778–785

35. Martinez-Garcia GR, Bachmann Th, Williams CJ, Burgoyne A, Edyvean RGJ (2006) Int Biodeterior Biodegrad 58:231–238
36. Saeed A, Akhter MW, Iqbal M (2005) Sep Purif Technol 45:25–31
37. Reza Sangi M, Shahmoradi A, Zolgharnein J, Azimi GH, Ghorbandoost M (2008) J Hazard Mater 155:513–522
38. Gomez del Rio JA, Morando PJ, Cicerone DS (2004) J Environ Manage 71:169–177
39. Elkabouss K, Kacimi M, Ziyad M, Bozon-Verduraz F (2005) J Phys IV 123:313–317
40. Al-Asheh S, Banat F, Mohai F (1999) Chemosphere 39:2087–2096
41. Hassan SSM, Awwad NS, Aboterika AHA (2008) J Hazard Mater 154:992–997
42. Xu Y, Wang DZ, Yang L, Tang HG (2001) Mater Charact 47:83–87
43. Ho YS, Wase DAJ, Forster CF (1996) Environ Technol 17:71–77
44. Sheng GD, Shao DD, Ren XM, Wang XQ, Li JX, Chen YX, Wang XK (2010) J Hazard Mater 178:505–516
45. Hu BW, Cheng W, Zhang H, Sheng GD (2010) J Radioanal Nucl Chem 285:389–398
46. Ren XM, Wang SW, Yang ST, Li JX (2010) J Radioanal Nucl Chem 283:253–259
47. Sheng GD, Hu J, Jin H, Yang ST, Ren XM, Li JX, Chen YX, Wang XK (2010) Radiochim Acta 98(5):291–299
48. Liao DX, Zheng W, Li XM, Yang Q, Yue X, Guo L, Zeng GM (2010) J Hazard Mater 177:126–130
49. Yüzer H, Kara M, Sabah E, Çelik MS (2008) J Hazard Mater 151:33–37
50. Fan QH, Shao DD, Wu WS, Wang XK (2009) Chem Eng J 150:188–195
51. Tan XL, Chen CL, Yu S, Wang XK (2008) Appl Geochem 23:2767–2777
52. Tan XL, Fan QH, Wang XK, Grambow B (2009) Environ Sci Technol 43:3115–3121
53. Fan QH, Tan XL, Li JX, Wang XK, Wu WS, Montavon G (2009) Environ Sci Technol 43(15):5776–5782
54. Xu D, Ning QL, Zhou X, Chen CL, Tan XL, Wu AD, Wang X (2005) J Radioanal Nucl Chem 266:419–424
55. Sheng GD, Wang SW, Hu J, Lu Y, Li JX, Dong YH, Wang XK (2009) Colloid Surf A 339:159–166
56. Yang ST, Li JX, Lu Y, Chen YX, Wang XK (2009) Appl Radiat Isot 67:1600–1608
57. Tan XL, Wang XK, Chen CL, Sun AH (2007) Appl Radiat Isot 65:375–381
58. Cotton F, Wilkinson G (1980) Advance inorganic chemistry. Wiley, New York
59. Esmadi F, Simm J (1995) Colloid Surf A 104:265–270
60. Xu D, Chen CL, Tan XL, Hu J, Wang XK (2007) Appl Geochem 22:2892–2906
61. LoPes MA, Monteiro FJ, Santos JD, Serro AP, Saramago B (1999) J Biomed Mater Res 45:370–375
62. Susuki T, Yamamoto T, Yoriyama M, Kameyama T (1997) J Biomed Mater Res 34:507–517
63. Tan XL, Wang XK, Geckeis H, Rabung Th (2008) Environ Sci Technol 42:6532–6537
64. Chen CL, Wang XK, Nagatsu M (2009) Environ Sci Technol 43:2362–2367
65. Xu D, Shao DD, Chen CL, Ren AP, Wang XK (2006) Radiochim Acta 94:97–102
66. Chen CL, Wang XK (2007) Appl Geochem 22:436–445
67. Li XL, Chen CL, Chang PP, Yu SM, Wu WS, Wang XK (2009) Desalination 244:283–292
68. Shao DD, Fan QH, Li JX, Niu ZW, Wu WS, Chen YX, Wang XK (2009) Micropor Mesopor Mater 123:1–9
69. Yang ST, Zhao DL, Zhang H, Lu SS, Chen L, Yu XJ (2010) J Hazard Mater 183:632–640
70. Hu J, Xu D, Chen L, Wang XK (2009) J Radioanal Nucl Chem 279:701–708
71. Hu J, Xie Z, He B, Sheng GD, Chen CL, Li JX, Chen YX, Wang XK (2010) Sci China B: Chem 53(6):1420–1428
72. Chang P, Yu S, Chen T, Ren A, Chen C, Wang X (2007) J Radioanal Nucl Chem 274:153–160
73. Chen CL, Wang XK, Jiang H, Hu WP (2007) Colloid Surf A 302:121–125
74. Guo ZQ, Xu DP, Zhao DL, Zhang SW, Niu HH, Chen ZS, Xu JZ (2010) J Radioanal Nucl Chem. doi:10.1007/s10967-010-0706-2
75. Shao DD, Jiang ZQ, Wang XK (2010) Plasma Process Polym 7(7):552–560
76. Shao DD, Sheng GD, Chen CL, Wang XK, Nagatsu M (2010) Chemosphere 79:679–685
77. Genc-Fuhrman H, Tjell JC, McConchie D (2004) Environ Sci Technol 38:2428–2434
78. Panday KK, Prasad G, Singh VN (1985) Water Res 19:869–873
79. Barrow NJ (1992) J Soil Sci 43:37–45
80. Tan XL, Hu J, Zhou X, Yu SM, Wang XK (2008) Radiochim Acta 96:487–495
81. Hu J, Shao DD, Chen CL, Sheng GD, Li JX, Wang XK, Nagatsu M (2010) J Phys Chem B 114:6779–6785
82. Sheng GD, Hu J, Wang XK (2010) Appl Radiat Isot 66:1313–1320
83. Sheng GD, Shao DD, Fan QH, Xu D, Chen YX, Wang XK (2009) Radiochim Acta 97:621–630